J Biomol NMR (2015) 61:287–298
DOI 10.1007/s10858-015-9897-8

ARTICLE

Action of the multifunctional peptide BP100 on native biomembranes examined by solid-state NMR

Julia Misiewicz · Sergii Afonin · Stephan L. Grage · Jonas van den Berg · Erik Strandberg · Parvesh Wadhwani · Anne S. Ulrich

Received: 3 November 2014 / Accepted: 10 January 2015 / Published online: 24 January 2015

Abstract Membrane composition is a key factor that regulates the destructive activity of antimicrobial peptides and the non-leaky permeation of cell penetrating peptides in vivo. Hence, the choice of model membrane is a crucial aspect in NMR studies and should reflect the biological situation as closely as possible. Here, we explore the structure and dynamics of the short multifunctional peptide BP100 using a multinuclear solid-state NMR approach. The membrane alignment and mobility of this 11 amino acid peptide was studied in various synthetic lipid bilayers with different net charge, fluidity, and thickness, as well as in native biomembranes harvested from prokaryotic and eukaryotic cells. ^{19}F-NMR provided the high sensitivity and lack of natural abundance background that are necessary to observe a labelled peptide even in protoplast membranes from *Micrococcus luteus* and in erythrocyte ghosts. Six selectively ^{19}F-labeled BP100 analogues gave remarkably similar spectra in all of the macroscopically oriented membrane systems, which were studied under quasi-native conditions of ambient temperature and full hydration. This similarity suggests that BP100 has the same surface-bound helical structure and high mobility in the different biomembranes and model membranes alike, independent of charge, thickness or cholesterol content of the system. ^{31}P-NMR spectra of the phospholipid components did not indicate any bilayer perturbation, so the formation of toroidal wormholes or micellarization can be excluded as a mechanism of its antimicrobial or cell penetrating action. However, ^{2}H-NMR analysis of the acyl chain order parameter profiles showed that BP100 leads to considerable membrane thinning and thereby local destabilization.

Keywords Solid-state ^{19}F-/^{31}P-/^{2}H-NMR · Model bilayers and native biomembranes · Antimicrobial and cell penetrating functions · Membrane thinning · BP100

J. Misiewicz · A. S. Ulrich (✉)
Institute of Organic Chemistry, Karlsruhe Institute of Technology (KIT), Fritz-Haber-Weg 6, 76131 Karlsruhe, Germany
e-mail: anne.ulrich@kit.edu

S. Afonin · S. L. Grage · J. van den Berg · E. Strandberg · P. Wadhwani · A. S. Ulrich
Institute of Biological Interfaces (IBG-2), Karlsruhe Institute of Technology (KIT), POB 3640, 76021 Karlsruhe, Germany

Introduction

The lipid environment constitutes more than a passive matrix for membrane proteins and membrane-associated peptides, but it can directly influence their function by controlling the molecular conformation, dynamics and state of oligomerization. In particular, the structural behaviour of membrane-active peptides is known to depend critically on the local environment. Due to their short sequence, their folding is strongly influenced by inter-molecular contacts with the surrounding molecules, and not just by intra-molecular interactions. Membrane-active peptides, as are frequently discussed as promising antibiotics and/or cell penetrating carriers, are usually unfolded in solution and tend to convert between different membrane-bound states, depending on lipid properties such as bilayer phase, membrane thickness or spontaneous curvature, or other environment parameters such as peptide concentration, pH or temperature (Afonin et al. 2008a, b, 2014; Bortolus et al. 2013; Cheng et al. 2009; Glaser et al. 2005; Grage et al. 2010; Islami et al. 2014; Matar and Besson 2011; Perrin et al. 2014; Strandberg et al. 2012, 2013; Yang et al. 2013).

Finding an appropriate membrane model therefore presents an important aspect in structural studies of membrane proteins and peptides. As laid out for example by Cross et al. the choice of membrane-mimicking environment has a significant impact on the structure of membrane proteins (Cross et al. 2013; Zhou and Cross 2013). Crystallography and liquid-state NMR are obviously restricted in the range of intrinsically suitable membrane-mimicking media. Detergent micelles are often chosen to obtain high-resolution 3D structures (Haney et al. 2009; Mäler 2012; Schrank et al. 2013), but flat bilayers are in many cases essential to represent a meaningful environment (Koch et al. 2012; Zhou and Cross 2013). Solid-state NMR analysis can be readily carried out on such macroscopically oriented membrane samples under quasi-native conditions, i.e. at ambient temperature and full hydration. In this approach, the lipid composition can be chosen essentially at will and thereby offers enormous flexibility in the range of systems that can be addressed, including native biomembranes. The use of oriented solid-state NMR methods may, however, tends to require more challenging labelling approaches and yields lower resolution and sensitivity than liquid-state NMR. Yet, the use of oriented membrane samples is particularly beneficial to decrease linewidth and obtain orientational constraints (Gopinath et al. 2013; Naito 2009).

To cope with the low sensitivity that is inherent to isotope labels such as ^{15}N or ^{13}C, we and others have intensively used ^{19}F-NMR to observe selectively ^{19}F-labelled peptides and smaller membrane proteins (Chen et al. 2013; Didenko et al. 2013; Koch et al. 2012; Kubyshkin et al. 2012; Marsh and Suzuki 2014; Ulrich 2005). With these methodological advances, even native membranes could be studied, e.g. the alignment of the antimicrobial peptides gramicidin S, PGLa and KIGAKI was determined in oriented protoplasts from *Micrococcus luteus* and in erythrocyte plasma membranes (Ieronimo et al. 2010; Koch et al. 2012; Wadhwani et al. 2013). Compared to model membrane constituted of synthetic phospholipids, the composition and layered structure of native biomembranes is much more complex, especially in view of the non-lipidic components like proteins and carbohydrates (Fig. 1a). Native membranes obviously represent the most relevant biological matrix, but studies in synthetic model bilayers are still beneficial for several reasons. Model systems allow simplifying the complex composition of native membranes, and to address a single specific aspect, such as the response of peptide alignment to spontaneous bilayer curvature, fluidity, or thickness (Afonin et al. 2008a, b; Afonin et al. 2014; Anbazhagan and Schneider 2010; De Planque et al. 2004; Grage et al. 2010; Muhle-Goll et al. 2012; Ouellet et al. 2007; Perrin et al. 2014; Yang et al. 2013; Strandberg et al. 2012, 2013). Furthermore, the handling and preparation of model bilayers is far easier than the elaborate isolation and preparation of oriented samples from native membranes, and extensive series of studies are often only feasible with model systems. The quality of alignment can be readily examined using ^{31}P-NMR of the phospholipid component, both in model bilayers as well as in native membranes. However, studies of the lipid response through established solid-state ^{2}H-NMR on deuterated lipids, as we have conducted here to evaluate membrane thinning effects, are very difficult to perform on biomembranes. It would require significant effort to obtain a per-deuterated biological membrane preparation that in addition contains no background from deuterated proteins.

In order to relate any results obtained in model bilayers to the actual biological system, a comparison of native and model membranes seems fundamentally important. Furthermore, the comparison of native membranes with a range of model bilayers differing in their physical properties should also give new insight into peptide function. By asking which model bilayers reflect the same or different behaviour of a peptide as in native membranes, should give clues on which aspect of the natural lipid environment determines the response to the peptide. Such evaluation of potential differences between model and biological membranes was the aim of this study, using the peptide BP100 as a representative for the class of amphipathic cationic peptides with pronounced membrane activity. As in previous studies, cell membranes from *M. luteus* and erythrocyte ghosts were used to represent prokaryotic and eukaryotic membranes, respectively, and we compared them with a selection of model bilayers with characteristic physical properties (see Fig. 1b). DLPC has particularly short saturated acyl chains (C12:0, lauroyl), a zwitterionic headgroup and moderate positive spontaneous curvature, so it forms very thin bilayers with a gel-to-fluid phase transition around −2 to 7 °C (Koynova and Caffrey 1998). DMPC possesses common saturated acyl chains (C14:0, myristoyl), a zwitterionic headgroup and slightly positive spontaneous curvature, and it forms bilayers of intermediate thickness with a gel-to-fluid phase transition around 24 °C (Koynova and Caffrey 1998). DMPG has saturated acyl chains (C14:0, myristoyl), a negatively charged headgroup and moderate positive spontaneous curvature, and when mixed with DMPC it forms bilayers of intermediate thickness with a gel-to-fluid phase transition around 24 °C (Findlay and Barton 1978). Mixtures of DMPC/DMPG are often used to mimic bacterial membranes, as they are known to be rich in anionic lipids. DErPC possesses unsaturated acyl chains (C22:1, erucoyl), a zwitterionic headgroup and moderate negative spontaneous curvature, and it forms very thick bilayers with a gel-to-fluid phase transition around 12 °C (Koynova and

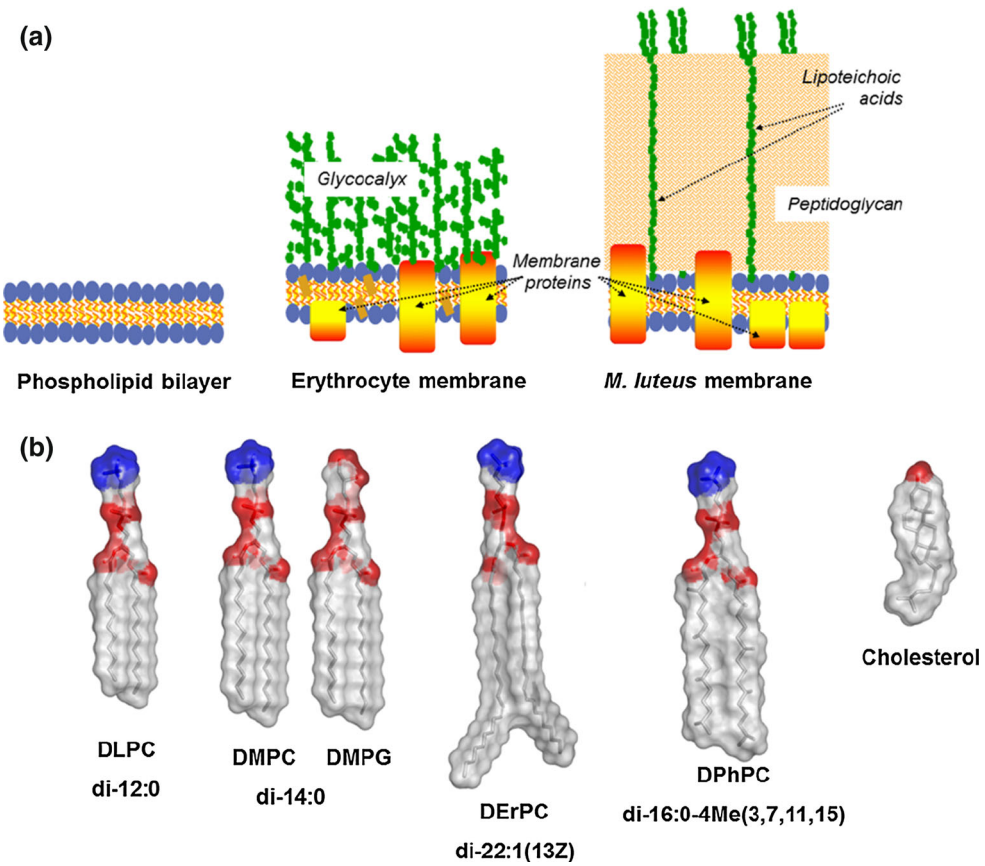

Fig. 1 Illustration of **a** the different membrane systems in which solid-state NMR was performed, and **b** the synthetic lipids used. Negatively charged parts of the lipid headgroups are colored in *red*, while positive charge is highlighted in *blue*

Caffrey 1998). DPhPC possesses tetramethylated (i.e. branched phytanoyl) saturated acyl chains, a zwitterionic headgroup and pronounced negative spontaneous curvature, and it forms highly stable bilayers of intermediate thickness with a gel-to-fluid phase transition below −120 °C (Lindsey et al. 1979); Cholesterol possesses a rigid, flat polycyclic core and modulates the membrane fluidity when incorporated into glycerophospholipid bilayers. Being the obligatory steroid component of animal membranes, it is often used in mixtures with DMPC, whose phase transition becomes completely abolished at concentrations up to 50 %.

The peptide BP100 [KKLFKKILKYL-NH_2] was chosen for the present study, because it has several properties considered to be necessary for membrane activity (Fig. 2). It possesses a pronounced amphipathic character when folded, with a net positive charge of +6 due to the presence of 5 lysine residues and the *N*-terminus (the *C*-terminus is amidated). It is unstructured in aqueous solution, but forms a well-defined α-helix when in contact with membranes (Wadhwani et al. 2014; Manzini et al. 2014). When embedded in DMPC/DMPG bilayers, BP100 was shown to align with the helix axis parallel to the membrane plane, such that the lysine-rich face points towards the aqueous surface and the hydrophobic face towards the bilayer core (Wadhwani et al. 2014). This orientation suggests a positioning of the peptide within the polar/apolar interface to match its amphipathic structure. Originally designed as an antimicrobial agent against plant pathogens, it has been found to actually possess numerous activities: Besides acting as antibiotic, it also acts as a cell penetrating carrier and facilitates intracellular transport (Eggenberger et al. 2011), and we have recently observed that it also promotes membrane fusion (Wadhwani et al. 2015). This multiple functionality might be based on a common underlying membrane activity. Remarkably, BP100 achieves this membrane activity with just 11 residues, which is significantly shorter than prominent examples of cationic α-helical antimicrobial peptides, such as cecropins, magainins, dermaseptins or cathelicidins (Yi et al. 2014; Jenssen et al. 2006; Kościuczuk et al. 2012; Zairi et al. 2009) with lengths of about 20 residues. Notably, BP100 as a helix is much too short to be able to span the typical width of a biological membrane, so it is unlikely to act as an oligomeric transmembrane pore. We have recently demonstrated for a series of related amphiphilic α-helical peptides that a minimum length is required to induce membrane damage in bacteria and erythrocytes, and that this threshold length corresponds to the bilayer thickness of lipid vesicles that were found to be ruptured by the peptides (Grau-Campistany et al. 2015).

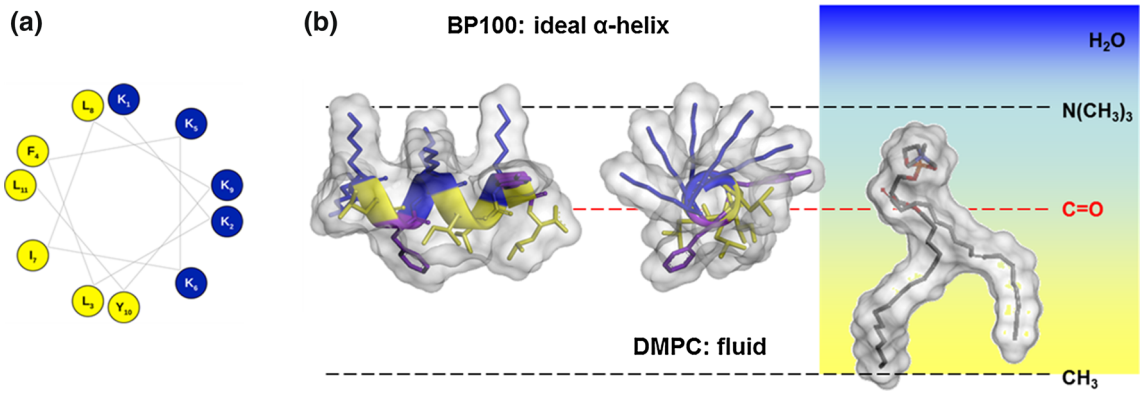

Fig. 2 BP100 is an unusually short (11 residues) cationic, amphipathic helical membrane-active peptide, with antimicrobial and cell penetrating function. **a** Helical wheel diagram with hydrophobic residues labelled in *yellow* and cationic ones in *blue*. **b** BP100 folded as an ideal α-helix compared to the dimensions of a DMPC monolayer in the fluid phase state. The solvent-accessibility surfaces (probe radius 1.4 Å) of the peptide and a lipid molecule taken from an MD simulation are displayed semi-transparent

Materials and methods

BP100 was synthesized using standard Fmoc-protocols, with a single *L*-3-CF_3-bicyclopent-[1.1.1]-1-yl glycine (CF_3-Bpg, obtained from Enamine Ltd., Kyiv, Ukraine) in the position of either Leu3, Phe4, Ile7, Leu8, Tyr10, or Leu11 (Table 1), as previously described (Wadhwani et al. 2014). Crude material post-cleavage was purified and analysed by a reverse-phase HPLC system equipped with a diode-array detector (Jasco Germany, Groß-Umstadt, Germany), with analytical (4.6 × 250 mm) and semipreparative (10 × 250 mm) C18 columns (Grace, Deerfeld, USA). Linear water-acetonitrile gradients were used (both eluents supplemented with 5 mM HCl to avoid any TFA background in ^{19}F-NMR), as described before (Afonin et al. 2003). The identity and purity of the products was confirmed by analytical reverse-phase HPLC and MALDI-TOF on the Autoflex III (Bruker Daltonics, Bremen, Germany).

The lipids 1,2-dilauroyl-*sn*-glycero-3-phosphatidylcholine (DLPC), 1,2-dimyristoyl-*sn*-glycero-3-phosphocholine (DMPC), 1,2-dimyristoyl-*sn*-glycero-3-phospho-(1′-rac-glycerol) sodium salt (DMPG), 1,2-diphytanoyl-*sn*-glycero-3-phosphocholine (DPhPC) and chain-deuterated analogues of DMPC and DMPG (DMPC-d_{54}, DMPG-d_{54}) were obtained from Avanti Polar Lipids (Alabaster, USA), cholesterol was purchased from Sigma-Aldrich Germany (Taufkirchen, Germany), while 1,2-dierucoyl-*sn*-glycero-3-phosphatidylcholine (DErPC) was obtained from NOF (Grobbendonk, Belgium). The lipids were stored as powders and used without further purification. All the other chemicals were of the highest purity available from either Roth (Karlsruhe, Germany) or Sigma-Aldrich.

Table 1 BP100 and ^{19}F-labeled analogues used in this study; structure of the label

Peptide	Sequence	CF_3-Bpg
BP100	KKLFKKILKYL-NH_2	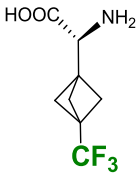
BP100-L3-Bpg	KK-*CF_3-Bpg*-FKKILKYL-NH_2	
BP100-F4-Bpg	KKL-*CF_3-Bpg*-KKILKYL-NH_2	
BP100-I7-Bpg	KKLFKK-*CF_3-Bpg*-LKYL-NH_2	
BP100-L8-Bpg	KKLFKKI-*CF_3-Bpg*-KYL-NH_2	
BP100-Y10-Bpg	KKLFKKILK-*CF_3-Bpg*-L-NH_2	
BP100-L11-Bpg	KKLFKKILKY-*CF_3-Bpg*-NH_2	

Oriented samples for solid-state NMR with the synthetic lipids were prepared as described before (Glaser et al. 2004; Wadhwani et al. 2012a). Briefly, peptide and lipid was co-dissolved in a mixture of water/methanol/chloroform, and equally distributed onto thin (ca. 0.08 mm) glass slides from Marienfeld (Lauda-Königshofen, Germany), dried under vacuum and re-hydrated at 48 °C in an atmosphere of 96 % relative humidity for 24 h (over saturated K_2SO_4). For ^{2}H-NMR measurements, deuterium-depleted water (Sigma-Aldrich Germany) was used for hydration to avoid background signal. Hydrated samples were wrapped in several layers of parafilm and a polyethylene foil to avoid dehydration, and were kept at −20 °C until use. Usually 0.2–0.9 mg of the ^{19}F-labeled peptide was used, and the lipid amounts were adjusted to get the desired peptide/lipid molar ratio.

Native membranes were prepared from human erythrocyte membranes and from *M. luteus* ATCC 4698 protoplasts as previously described (Ieronimo et al. 2010; Koch et al. 2012). Human blood suspensions, obtained from the Karlsruhe municipal hospital, were lysed and repeatedly washed to yield erythrocyte ghosts. Membranes of *M. luteus* (from the German Collection of Microorganisms and Cell Cultures, Braunschweig, Germany) were isolated after

treatment with lysozyme purchased from Fluka (Buchs, Switzerland). The phospholipid content was determined by standard colorimetric phosphate assay (Ames 1966) using Folch extracts (Folch et al. 1957) from fresh membrane preparations. To reconstitute the membrane suspensions with peptides, they were washed with tenfold excess of Millipore Milli-Q water, supplemented with 0.005 % NaN_3 (18,000×*g*, 90 min at 4 °C), on an Avanti J-25 centrifuge (Beckman, Krefeld, Germany). Appropriate amounts of peptide (usually 0.5 mg, aiming at a peptide/lipid molar ratio of 1/20) were co-agitated for 2 h with the membrane suspensions. To prepare oriented NMR samples, the material was equally distributed onto Marienfeld glass slides and dried under gentle sterile air flow (14–20 h). The slides were stacked and re-hydrated at 96 % relative humidity at 48 °C (14–20 h). The wrapped samples were stored at −20 °C until use.

Solid-state NMR spectra were acquired on a Bruker Avance 500 MHz spectrometer operating at 470.6 MHz (^{19}F), at 202.5 MHz (^{31}P), and at 76.7 MHz (^{2}H) (Bruker Biospin, Karlsruhe, Germany). Double-tuned goniometer-equipped ^{19}F/^{1}H probes (from Doty Scientific, Columbia, USA, and a home-built probe) were employed for ^{19}F-NMR, and flat-coil double-resonance ^{1}H/X probes were employed for ^{31}P-NMR and ^{2}H-NMR (Bruker in collaboration with KIT). Solid-state ^{19}F-NMR measurements were performed as previously described in detail (Ieronimo et al. 2010). Samples were placed such that the membrane normal was collinear to external magnetic field. ^{19}F-NMR experiments employed an ARING sequence for background suppression (Zhang et al. 1990). A Hahn-echo pulse sequence was used for ^{31}P-NMR with a 90°-pulse length of 5–8 µs and an echo time of 25–30 µs. ^{2}H-NMR was performed using a solid echo sequence with a 90° pulse length of 4.2 µs, an echo time of 30 µs and a relaxation delay of 0.5 s (Davis et al. 1976). In all ^{19}F-NMR and ^{31}P-NMR experiments Two Pulse Phase Modulation (TPPM) ^{1}H-decoupling was employed. The ^{19}F-NMR spectra were referenced by sample replacement using an aqueous solution of 100 mM NaF, the resonance of which was set to −119.5 ppm at 35 °C (Glaser and Ulrich 2003). For ^{31}P-NMR spectra calibration, 85 % H_3PO_4 was used as reference substance. About 30,000–50,000 scans, 200–500 scans and 1,000–10,000 scans were averaged for ^{19}F-, ^{31}P- and ^{2}H-NMR spectra, respectively. Spectra were processed with standard tools of the TopSpin software from Bruker.

Unless stated otherwise, BP100 was reconstituted into native biomembranes and into DMPC/cholesterol at a peptide/lipid molar ratio of 1/20, and into all other model membranes at a peptide/lipid molar ratio of 1/100. All NMR measurements on model membranes were performed above the phase transition temperature, i.e. the experiments on DPhPC samples at 15 °C, on DMPC/cholesterol samples at 40 °C, and on DMPC/DMPG (3:1), DLPC as well as DErPC samples at 35 °C. Native biomembrane samples were measured at 40 °C.

Results

The quality of alignment of oriented membrane samples for solid-state NMR is conveniently characterized by observing the ^{31}P-NMR signal of the phospholipids. For model membranes, the standard sample preparation procedure for oriented samples relies on spreading a co-dissolved peptide/lipid mixture in organic solvents onto glass plates, which generally leads to a high degree of alignment. Indeed, the ^{31}P-NMR spectra (Fig. 3a) show a sharp signal around 30 ppm, which is indicative of phospholipids aligned along the membrane normal, indicating that most model bilayers (DLPC, DMPC/DMPG, DErPC and DPhPC) were well oriented. Only the DMPC/cholesterol samples showed broader ^{31}P-NMR lines and an additional signal from non-oriented lipid near −20 ppm, suggesting poorer orientation (Fig. 3a, lowest trace). The native biomembrane preparations, where the peptide is added to an aqueous suspension of vesicles, however, varied in their degree of lipid alignment (Fig. 3b, c). While in oriented erythrocyte membranes, a fairly high degree of orientation was observed (Fig. 3b), the spectra of protoplasts exhibit broadening due to a pronounced mosaic spread, plus an

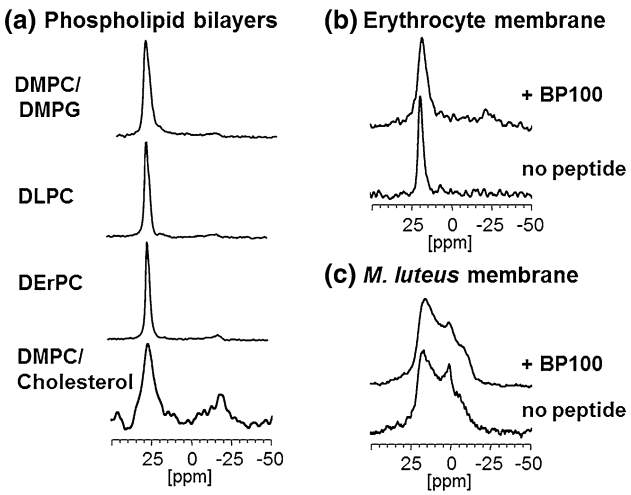

Fig. 3 ^{31}P-NMR spectra reflect the quality of alignment of the oriented lipid bilayers and show the influence of BP100. **a** Representative ^{31}P-NMR spectra of selected model membranes containing the BP100-Y10-Bpg peptide, measured well above the gel-to-fluid phase transition temperature. Amongst the model membranes, only the DMPC/cholesterol systems showed a deviation from otherwise high-quality alignments. Oriented native membranes of erythrocytes **(b)** and *M. luteus* **(c)**, in the presence (**b**, **c**, upper traces) and absence (**b**, **c**, lower traces) of BP100

additional sharp signal at the isotropic ^{31}P chemical shift of the phospholipids (Fig. 3c). The broadening probably stems from the membrane proteins, which are highly abundant in membranes of bacteria. Though certainly more than 50 % of the lipids are oriented, an exact estimation of the degree of alignment remains difficult. As previously observed (Ieronimo et al. 2010; Koch et al. 2012), the spectra did not allow discriminating any individual lipid species, as in all cases they appeared as one broad signal. The second, isotropic ^{31}P-NMR signal may be attributed to entrapped inorganic phosphate or phosphates on the membrane exoskeleton, i.e. they could be of non-lipidic origin or rather represent a small fraction of non-lamellar lipid morphologies. In the native membrane samples we observed ^{31}P-NMR CSA values (measured between both edges of the lineshape) of about 40 ppm for erythrocytes and 30 ppm for the bacterial membranes. Both values are significantly lower than typical ^{31}P-NMR spectral widths of synthetic phospholipids (e.g. 47 ppm for DMPC). Nonetheless, we can conclude that the peptide does not perturb the membrane severely in either preparation, since the addition of peptide only lead to a marginal broadening even at a peptide/lipid molar ratio of 1/20.

Based on the good quality of the oriented samples, we proceeded to examine the structure of BP100 in the various types of bilayers using solid-state ^{19}F-NMR, as summarized in the Fig. 4. The spectra exhibit characteristic triplets due to the ^{19}F–^{19}F dipolar coupling within the CF_3-group of the employed CF_3-Bpg label. We note at this point, that the components of the triplet are influenced differently by broadening due to mosaic spread, which often leads to a deviation from the expected 1:2:1 triplet lineshape. From the splitting values of several peptide analogues—each one labelled in a different single position—the conformation and alignment of a membrane-bound peptide can be determined (Koch et al. 2012; Kubyshkin et al. 2012; Ulrich 2005). A comprehensive ^{19}F-NMR analysis of BP100 in DMPC/DMPG (3:1) model membranes, using the very same set of peptides as in this study, has been recently published (Wadhwani et al. 2014). In that study we concluded that BP100 is folded as a helix and lies flat on the bilayer surface, with the helix axis parallel to the membrane plane and the azimuthal rotation just as expected from the amphiphilic profile (see Fig. 2). A careful dynamical evaluation of the ^{19}F-data had also revealed that BP100 is highly mobile in DMPC/DMPG, undergoing not only fast lateral rotation but also wobbling extensively along its helix axis (Wadhwani et al. 2014). Here, we simply use the obtained series of spectra as an indicator of peptide alignment, structure and dynamics, in order to monitor any possible membrane-dependent differences. The set of sampled positions, (positions 3, 4, 7, 8, 10, 11) covers all uncharged residues of the BP100 sequence, thereby allowing such comparison over the entire length of the peptide.

It can be readily seen (Fig. 4) that in four cases, DMPC/DMPG, DLPC, DErPC and DPhPC, all spectra corresponding to each of the labelling positions are virtually identical, despite the differences in membrane charge, thickness and fluidity. Only in the DPhPC bilayers, an

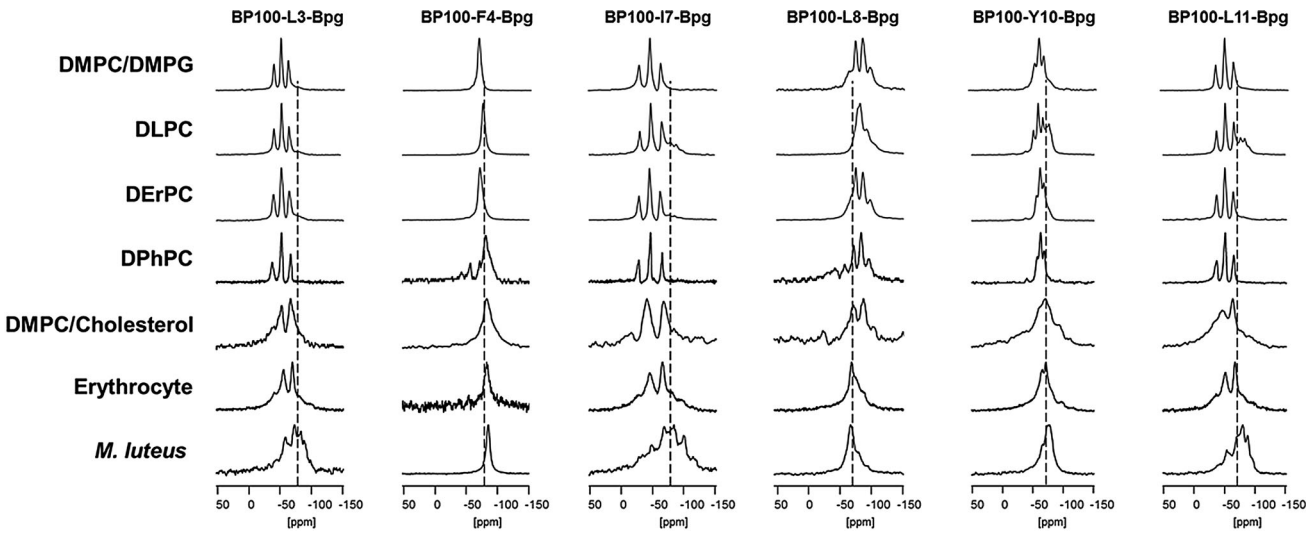

Fig. 4 ^{19}F-NMR spectra of CF_3-labelled BP100 analogues reconstituted in different oriented membrane systems. *Each column* shows the ^{19}F-NMR spectra of BP100 labelled in the particular position indicated. *Dashed lines* indicate the isotropic ^{19}F chemical shift. All model bilayer samples were measured well above their respective gel-to-fluid phase transition temperatures, and the biomembrane samples were measured at 313 K. The peptide/lipid molar ratio was 1/100 for DMPC/DMPG, DLPC, DErPC and DPhPC, and 1/20 for DMPC/cholesterol, erythrocytes and *M. luteus* samples

additional minor component contributing about 30 % of the signal is observed in the peptides labelled at positions 4 and 8. Since all peptides were prepared as single batches, a contamination is unlikely, so these signals may originate from a minor fraction of molecules oriented differently. The ^{19}F-NMR spectra in DMPC/Cholesterol differ from all other model membranes in that they are significantly broadened. This degree of broadening correlates well with the poorest quality of lipid alignment observed in the ^{31}P-NMR spectra among all studied model membranes (lowest row in Fig. 3a). Even in the presence of an additional broad powder component, all principal splittings (except for BP100-I7-Bpg) are essentially the same as in the other model membranes.

Remarkably, the ^{19}F-NMR spectra obtained from the two native biomembranes of erythrocytes and *M. luteus* (two lowest rows in Fig. 4) reproduce the signals of the model bilayers rather well. Even though they differ significantly in linewidth from most of the model membrane data, all triplets in the native membranes match the respective signals in the model systems. The spectra obtained in *M. luteus* spectra contain significant powder contributions from non-oriented membrane regions, is full agreement with the largest mosaic spread seen in the ^{31}P-NMR spectra (Fig. 3c). Such high heterogeneity is in fact anticipated here, because the amount of non-lipidic components in these bacterial membranes is the greatest.

The similarity of the corresponding ^{19}F-NMR spectra across all lipid systems becomes even more evident when comparing the splitting of the triplets (Fig. 5). Even though the splitting values vary fundamentally between the different labelling positions, similar values are found when comparing the splittings from the same labelling position in different lipid systems. Despite some outliers, the overall pattern of dipolar couplings along peptide helix remains intact. This remarkable similarity strongly suggests that BP100 does not change its orientation, mobility or structure within the entire set of the membranes tested.

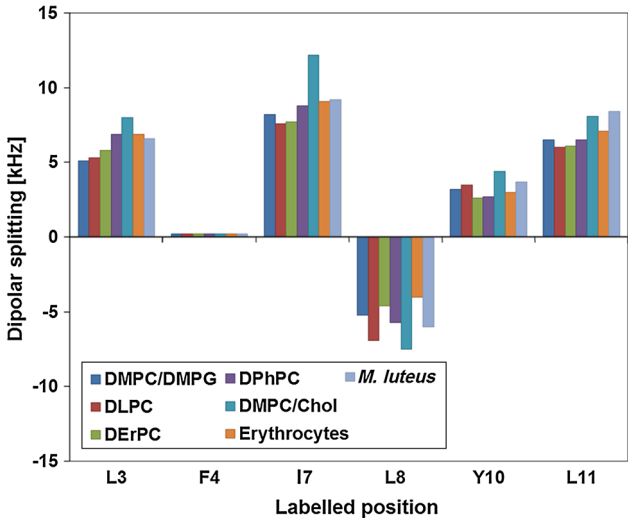

Fig. 5 Distribution of ^{19}F–^{19}F dipolar couplings of the CF_3-labels measured for each substituted position along the BP100 sequence in different membrane systems. The error of each dipolar coupling value is ~1 kHz, as estimated from the linewidth

The orientation of BP100 in fluid DMPC/DMPG bilayers has been analysed previously in detail using ^{19}F-NMR, ^{15}N-NMR and oriented circular dichroism, showing a helix alignment parallel to the membrane surface (Wadhwani et al. 2014). Peptides in such an alignment, which fits very well in the polar/apolar interface of the bilayer, have been discussed to act on lipid bilayers by membrane thinning (Grage et al. 2010; Huang 2006; Mecke et al. 2005; Neale et al. 2014; Su et al. 2013). Such influence on membrane thickness can be readily examined by measuring the lipid chain order, because membrane thickness is directly related to the conformational freedom of the acyl chain segments. Solid-state ^{2}H-NMR on chain-deuterated lipid provides a means to access lipid chain order, as membrane thinning would decrease the order parameters of the labelled acyl chains, which in turn becomes apparent as a reduction in the observed quadrupolar splitting (Petrache et al. 2000). We thus evaluated the effect of BP100 on either component of a DMPC/DMPG mixture, by preparing two sets of bilayers containing BP100, where either DMPC or DMPG was chain-deuterated (Fig. 6a, b, respectively). Indeed, with increasing peptide/lipid molar ratio we observed a significant reduction of the quadrupolar splittings of the deuterated segments in both cases. For chain-deuterated DMPC-d_{54} at a peptide/lipid molar ratio of 1/25, the largest splitting (corresponding to carbons closest to the head group) are reduced to about 86 % of the value without BP100, and the smallest splitting (corresponding to the methyl group) is reduced to around 72 %. For chain-deuterated DMPG-d_{54}, the effect is even bigger, with corresponding reductions of around 83 and 70 %.

Discussion and conclusions

We have recently determined the orientation of the antimicrobial and cell penetrating peptide BP100 (Fig. 2) in DMPC/DMPG bilayers, using ^{19}F- and ^{15}N-NMR and oriented circular dichroism (Wadhwani et al. 2014). There, we found that the peptide helix is oriented essentially flat on the membrane surface, and no change in the ^{19}F-NMR splittings was observed for peptide/lipid molar ratios ranging from 1/10 to 1/3,000 (Wadhwani et al. 2014). Those data suggested that the peptide is monomeric throughout, with no sign of any concentration dependent

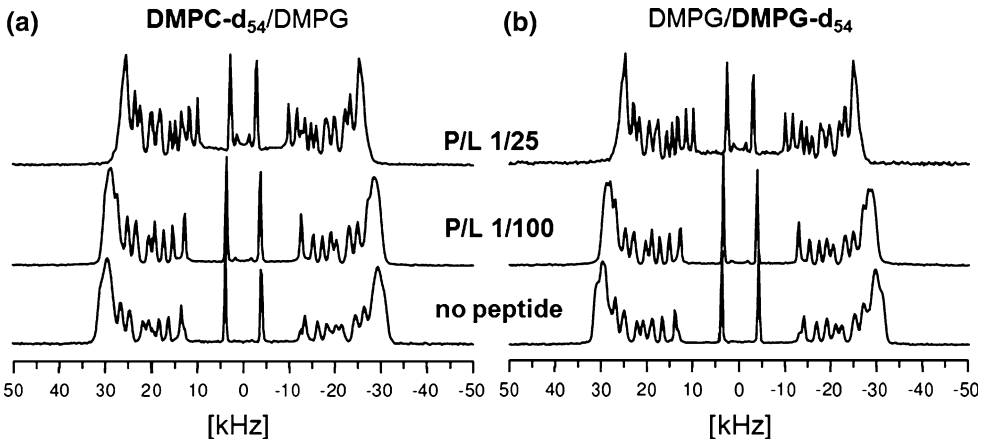

Fig. 6 Concentration-dependent thinning of model membranes induced by BP100. ^{2}H-NMR spectra of deuterated lipids in oriented samples of DMPC-d_{54}/DMPG (**a**), and in DMPC/DMPG-d_{54} (**b**), with peptide/lipid molar ratios as indicated

re-alignment or oligomerization. The present study thus addresses the behavior of BP100 in a wide range of different membrane systems, covering native biomembranes of prokaryotic and eukaryotic cells, as well as model bilayers varying in charge, fluidity and thickness (Fig. 1). Our initial aim was to find any lipids that would influence the peptide structure and alignment, as these conditions should be relevant to understand the interaction between the multifunctional BP100 and different types of cellular membranes. Specific attention was paid to native biomembranes, expecting that they would be most informative and reveal some insight into the molecular mechanism of membrane perturbation, permeation and/or permeabilization.

Solid-state ^{19}F-NMR experiments in oriented membranes yield direct orientational information about the selectively labelled molecular segment. The splitting of each CF_3-label is indicative of the orientation of the labelled residue on the peptide, and on the local mobility as expressed, e.g., by an order parameter. Due to the rigid connection of the CF_3-group to the peptide backbone, this orientational and mobility information can be transferred to the overall peptide scaffold. A series of peptide analogues, each labelled at a different position, together then encode the orientation of the entire backbone with respect to the membrane. Moreover, the set of NMR data is also sensitive to the secondary structure and the dynamics of the peptide (Koch et al. 2012; Kubyshkin et al. 2012; Ulrich 2005). This way, the examination of six labelled positions provides a detailed picture of the conformation, alignment and dynamics of BP100 in the membrane-bound state. A striking similarity in the CF_3-group dipolar couplings of corresponding labels was found in all of the studied membrane systems, which implies that BP100 remains essentially unchanged in all three aspects, secondary structure, dynamics and orientation with respect to the bilayer.

The fact that the ^{19}F-NMR signals (Fig. 4, lowest row) appear very broad in *M. luteus* membranes can be readily explained. As evident from the ^{31}P-NMR spectra (Fig. 3c), which reflect the dispersion in the alignment of the phospholipids, a much wider distribution of membrane orientations is present in the samples of BP100 in *M. luteus*, giving rise to a broadening in the ^{19}F-NMR spectra as well. In the case of erythrocyte membranes, the ^{31}P-NMR spectra (Fig. 3b) show a lower mosaic spread, which is compatible with that of typical model membranes. The linewidth of the triplet peaks in the ^{19}F-NMR spectra of erythrocyte membranes is also narrower than in the case of *M. luteus*, though it is still broader than in most model membranes. This broadening, observed in both ^{31}P- and ^{19}F-NMR, may be due to other constituents of the native membranes that interfere with a uniform mode of binding of BP100 and lead to a more heterogeneous behaviour of the peptide. The high density of membrane proteins in bacterial membranes of *M. luteus* as compared to eukaryotic erythrocytes may thus explain that the largest broadening was indeed observed in *M. luteus* samples. The linewidths of both ^{31}P and ^{19}F-NMR spectra of the erythrocyte samples compare well with those of the DMPC/cholesterol samples, which may be due to the presence of cholesterol in both cases. Such similarity of erythrocyte and cholesterol-containing model membranes has been reported before (Koch et al. 2012).

Despite differences in linewidth, the values of the dipolar splittings compare remarkably well between the different membrane systems, showing that BP100 is largely unaffected by changes in the lipid composition. This finding is rather unexpected, as in many membrane-bound peptides a re-alignment is observed when changing the physical properties of the membrane. Considerable changes in the helix tilt angle have been reported, for example, in the transmembrane helix of PDGFR-β receptor upon varying membrane thickness (Muhle-Goll et al. 2012), but BP100 does not differ in thin DLPC compared to thick

DErPC. A variable extent of binding—depending on the charge of the membrane—has also been observed for cationic peptides such as PGLa (Tremouilhac et al. 2006; Grau-Campistany et al. 2015), but it does not seem to affect BP100. Furthermore, it had been conceived that the highly branched DPhPC or the sealed DMPC/cholesterol systems might promote or prevent BP100 insertion, but again this was not evident from the ^{19}F-NMR analysis in this study. Another fundamental feature of lipid bilayers concerns their spontaneous curvature, e.g. DLPC has a positive spontaneous curvature while DPhPC has a highly negative value. This property has been recently demonstrated to be a key factor that determines the insertion and tilt angle of various amphiphilic peptides in model membranes (Strandberg et al. 2012, 2013; Afonin et al. 2014), however, it does not affect BP100. Moreover, many cationic amphiphilic α-helices have been found to exhibit a distinct re-alignment behaviour as a function of peptide concentration. At concentrations below a characteristic threshold peptide/lipid ratio (mol/mol), these helices adopt an alignment parallel to the membrane surface, whereas they tilt and insert more deeply into the membrane at higher concentration (Grage et al. 2010). For BP100, however, such concentration-dependent re-alignment has never been observed. In our recent study of BP100 in DMPC/DMPG bilayers covering peptide/lipid molar ratios from 1/3,000 to 1/10, BP100 was always found to be exclusively oriented parallel to the membrane surface. The only change as a function of peptide/lipid molar ratio as well as membrane charge has been reported in a recent study (Manzini et al. 2014), where BP100 was found to perturb DMPC/DMPG membranes above a very high peptide/lipid molar ratio of roughly 1/5, and in the presence of very high DMPG contents.

The insensitivity of BP100 to the physical properties of the membrane must lie in an interaction of the peptide with a region of the lipid bilayer that is common to all membranes. The unusually short peptide BP100 with only 11 amino acids (5 lysines, 6 hydrophobic residues) cannot insert deeply into the membrane, but should reside within the headgroup region, which in all cases consists of glycerophosphates. As illustrated in Fig. 2, the dimensions of the baseball-shaped BP100 (given its helix diameter and length) would fit nicely within the headgroup region of a bilayer. The amphiphilic headgroup regions of all membranes studied so far may thus be similar enough to lead to the same non-specific peptide-lipid interactions in all cases. Nevertheless, we know that BP100 binds tightly and in a discrete alignment (at least in oriented bilayers without excess water), because the dipolar couplings reach relatively high values (up to $\sim$12 kHz depending on label orientation). The partial averaging of the dipolar ^{19}F-NMR couplings has been evaluated in terms of a highly dynamical state of BP100 (Wadhwani et al. 2014), whose extensive wobble is not surprising in view of its compact shape.

A location of BP100 in the headgroup region, embedded with the helix axis parallel to the membrane surface such as to match the polar/apolar interface of the bilayer, would also explain the observed membrane thinning very well (Fig. 6). Membrane thinning has been recently proposed for BP100 by Manzini et al. for similar experimental conditions (peptide/lipid molar ratio and DMPG content) as used in our study (Manzini et al. 2014). This effect on membrane thickness has been discussed intensively as a possible mode of action of amphiphilic peptides on lipid bilayers (Grage et al. 2010; Huang 2006; Mecke et al. 2005; Neale et al. 2014; Su et al. 2013). By requiring more space in the headgroup region, peptides that are embedded in the upper membrane region will lead to a lateral spreading of the lipid acyl chains. This in turn leads to thinning of the membrane, such that the volume-per-lipid stays constant within the incompressible bilayer. A manifestation of such thinning now allows conclusions on the mechanism of membrane-activity. Amongst several modes of activity discussed for α-helical antimicrobial peptides, this scenario corresponds to the "carpet" mechanism of peptide-induced membrane perturbation (Shai 1999). We indeed observed clear indications of membrane thinning in our ^{2}H-NMR analyses of chain deuterated mixed DMPC/DMPG bilayers, where the addition of BP100 lead to a reduction in quadrupolar splittings and hence in acyl chain order. Moreover, we observed a somewhat stronger effect of the cationic BP100 on anionic DMPG than on zwitterionic DMPC. This subtle difference when comparing charged lipids versus zwitterionic ones might be taken to imply a potential for lipid-induced clustering, as discussed for many cationic amphipathic peptides (Wadhwani et al. 2012b; Epand et al. 2010a, b). Recently, however, BP100 was found to exhibit only a moderate propensity for clustering of phosphatidylglycerol lipids (Wadhwani et al. 2012b). Furthermore, strong clustering would not be compatible either with the relatively strong thinning effect observed on the DMPC component in the mixture, and would thus not agree with the common picture of thinning being most effectively induced by single peptides rather than by peptide clusters (Huang 2006).

In summary, in this multinuclear solid-state NMR study we have demonstrated with selectively ^{19}F-labeled peptides that structural studies on oriented samples can be readily extended from model bilayers to native biomembranes. By cross-comparing biological membranes with a range of model membranes, using also ^{31}P- and ^{2}H-NMR, we obtained new insights about the invariant peptide-lipid interactions of BP100. In particular, we could confirm that this short peptide can form a "carpet" on a variety of

membranes, ranging from model bilayers to native membranes, which as a consequence leads to membrane thinning. Mechanistic similarities and differences in the ultimate process of membrane permeabilization during antimicrobial action, or during the non-leaky peptide transfer across membranes, however, still need to be explored further (Wang et al. 2014; Wadhwani et al. 2015).

Acknowledgments We acknowledge A. Eisele and K. Scheubeck (KIT) for the technical support with peptide synthesis, R. A. M. Ciriello, C. Mink (KIT) for participation in the NMR measurements, P. K. Mykhailiuk and I. V. Komarov (University of Kyiv) for custom-synthesis of the amino acid CF_3-Bpg. This research was supported by the DFG-Center for Functional Nanostructures (E1.2).

References

Afonin S, Glaser RW, Berditchevskaia M, Wadhwani P, Gührs KH, Möllmann U, Perner A, Ulrich AS (2003) 4-Fluorophenylglycine as a label for ^{19}F NMR structure analysis of membrane-associated peptides. ChemBioChem 4:1151–1163. doi:10.1002/cbic.200300568

Afonin S, Grage SL, Ieronimo M, Wadhwani P, Ulrich AS (2008a) Temperature-dependent transmembrane insertion of the amphiphilic peptide PGLa in lipid bilayers observed by solid state ^{19}F NMR spectroscopy. J Am Chem Soc 130:16512–16514. doi:10.1021/ja803156d

Afonin S, Dürr UH, Wadhwani P, Salgado J, Ulrich AS (2008b) Solid state NMR structure analysis of the antimicrobial peptide gramicidin S in lipid membranes: concentration-dependent realignment and self-assembly as a β-Barrel. Top Curr Chem 273:139–154. doi:10.1007/128_2007_20

Afonin S, Glaser RW, Sachse C, Salgado J, Wadhwani P, Ulrich AS (2014) ^{19}F NMR screening of unrelated antimicrobial peptides shows that membrane interactions are largely governed by lipids. Biochim Biophys Acta 1838:2260–2268. doi:10.1016/j.bbamem.2014.03.017

Ames BN (1966) Assay of inorganic phosphate, total phosphate and phosphatases. In: Neufeld E, Ginsburg V (eds) Methods in enzymology, vol VIII., Complex CarbohydratesAcademic Press, New York, pp 115–118

Anbazhagan V, Schneider D (2010) The membrane environment modulates self-association of the human GpA TM domain-implications for membrane protein folding and transmembrane signaling. Biochim Biophys Acta 1798:1899–1907. doi:10.1016/j.bbamem.2010.06.027

Bortolus M, De Zotti M, Formaggio F, Maniero AL (2013) Alamethicin in bicelles: orientation, aggregation, and bilayer modification as a function of peptide concentration. Biochim Biophys Acta 1828:2620–2627. doi:10.1016/j.bbamem.2013.07.007

Chen H, Viel S, Ziarelli F, Peng L (2013) ^{19}F NMR: a valuable tool for studying biological events. Chem Soc Rev 42:7971–7982. doi:10.1039/c3cs60129c

Cheng JT, Hale JD, Elliot M, Hancock RE, Straus SK (2009) Effect of membrane composition on antimicrobial peptides aurein 2.2 and 2.3 from Australian southern bell frogs. Biophys J 96:552–565. doi:10.1016/j.bpj.2008.10.012

Cross TA, Murray DT, Watts A (2013) Helical membrane protein conformations and their environment. Eur Biophys J 42:731–755. doi:10.1007/s00249-013-0925-x

Davis JH, Jeffrey KR, Bloom M, Valic MI, Higgs TP (1976) Quadrupolar echo deuteron magnetic resonance spectroscopy in ordered hydrocarbon chains. Chem Phys Lett 42:390–394

de Planque MR, Rijkers DT, Liskamp RM, Separovic F (2004) The αM1 transmembrane segment of the nicotinic acetylcholine receptor interacts strongly with model membranes. Magn Reson Chem 42:148–154. doi:10.1002/mrc.1326

Didenko T, Liu JJ, Horst R, Stevens RC, Wüthrich K (2013) Fluorine-19 NMR of integral membrane proteins illustrated with studies of GPCRs. Curr Opin Struct Biol 23:740–747. doi:10.1016/j.sbi.2013.07.011

Eggenberger K, Mink C, Wadhwani P, Ulrich AS, Nick P (2011) Using the peptide BP100 as a cell-penetrating tool for the chemical engineering of actin filaments within living plant cells. ChemBioChem 12:132–137. doi:10.1002/cbic.20100040221

Epand RM, Epand RF, Arnusch CJ, Papahadjopoulos-Sternberg B, Wang G, Shai Y (2010a) Lipid clustering by three homologous arginine-rich antimicrobial peptides is insensitive to amino acid arrangement and induced secondary structure. Biochim Biophys Acta 1798:1272–1280. doi:10.1016/j.bbamem.2010.03.012

Epand RF, Maloy WL, Ramamoorthy A, Epand RM (2010b) Probing the "charge cluster mechanism" in amphipathic helical cationic antimicrobial peptides. Biochemistry 49:4076–4084. doi:10.1021/bi100378m

Findlay EJ, Barton PG (1978) Phase behavior of synthetic phosphatidylglycerols and binary mixtures with phosphatidylcholines in the presence and absence of calcium ions. Biochemistry 17:2400–2405. doi:10.1021/bi00605a023

Folch J, Lees M, Sloane Stanley GH (1957) A simple method for the isolation and purification of total lipides from animal tissues. J Biol Chem 226:497–509

Glaser RW, Ulrich AS (2003) Susceptibility corrections in solid-state NMR experiments with oriented membrane samples. Part I: applications. J Magn Reson 164:104–114. doi:10.1016/S1090-7807(03)00207-6

Glaser RW, Sachse C, Dürr UH, Wadhwani P, Ulrich AS (2004) Orientation of the antimicrobial peptide PGLa in lipid membranes determined from ^{19}F-NMR dipolar couplings of 4-CF_3-phenylglycine labels. J Magn Reson 168:153–163. doi:10.1016/j.jmr.2004.02.008

Glaser RW, Sachse C, Dürr UH, Wadhwani P, Afonin S, Strandberg E, Ulrich AS (2005) Concentration-dependent realignment of the antimicrobial peptide PGLa in lipid membranes observed by solid-state ^{19}F-NMR. Biophys J 88:3392–3397. doi:10.1529/biophysj.104.056424

Gopinath T, Mote KR, Veglia G (2013) Sensitivity and resolution enhancement of oriented solid-state NMR: application to membrane proteins. Prog Nucl Magn Reson Spectrosc 75:50–68. doi:10.1016/j.pnmrs.2013.07.004ì

Grage SL, Afonin S, Ulrich AS (2010) Dynamic transitions of membrane-active peptides. Methods Mol Biol 618:183–207. doi:10.1007/978-1-60761-594-1_13

Grau-Campistany A, Strandberg E, Wadhwani P, Reichert J, Bürck J, Rabanal F, Ulrich AS (2015) Hydrophobic mismatch demonstrated for membranolytic peptides, and their use as molecular rulers to measure bilayer thickness in native cells (in preparation)

Haney EF, Hunter HN, Matsuzaki K, Vogel HJ (2009) Solution NMR studies of amphibian antimicrobial peptides: linking structure to function? Biochim Biophys Acta 1788:1639–1655. doi:10.1016/j.bbamem.2009.01.002

Huang HW (2006) Molecular mechanism of antimicrobial peptides: the origin of cooperativity. Biochim Biophys Acta 1758:1292–1302. doi:10.1016/j.bbamem.2006.02.001

Ieronimo M, Afonin S, Koch K, Berditsch M, Wadhwani P, Ulrich AS (2010) ^{19}F NMR analysis of the antimicrobial peptide PGLa bound to native cell membranes from bacterial protoplasts and human erythrocytes. J Am Chem Soc 132:8822–8824. doi:10.1021/ja101608z

Islami M, Mehrnejad F, Doustdar F, Alimohammadi M, Khadem-Maaref M, Mir-Derikvand M, Taghdir M (2014) Study of orientation and penetration of LAH4 into lipid bilayer membranes: pH and composition dependence. Chem Biol Drug Des 84:242–252. doi:10.1111/cbdd.12311

Jenssen H, Hamill P, Hancock RE (2006) Peptide antimicrobial agents. Clin Microbiol Rev 19:491–511. doi:10.1128/CMR.00056-05

Koch K, Afonin S, Ieronimo M, Berditsch M, Ulrich AS (2012) Solid-state ^{19}F-NMR of peptides in native membranes. Top Curr Chem 306:89–118. doi:10.1007/128_2011_162

Kościuczuk EM, Lisowski P, Jarczak J, Strzałkowska N, Jóźwik A, Horbańczuk J, Krzyżewski J, Zwierzchowski L, Bagnicka E (2012) Cathelicidins: family of antimicrobial peptides—a review. Mol Biol Rep 39:10957–10970. doi:10.1007/s11033-012-1997-x

Koynova R, Caffrey M (1998) Phases and phase transitions of the phosphatidylcholines. Biochim Biophys Acta 1376:91–145. doi:10.1016/S0304-4157(98)00006-9

Kubyshkin VS, Komarov IV, Afonin S, Mykhailiuk PK, Grage SL, Ulrich AS (2012) Trifluoromethyl-substituted α-amino acids as solid state ^{19}F-NMR labels for structural studies of membrane-bound peptides. In: Gouverneur V, Müller K (eds) Fluorine in pharmaceutical and medicinal chemistry: from biophysical aspects to clinical applications. Imperial College Press, London, pp 91–138

Lindsey H, Petersen NO, Chan SI (1979) Physicochemical characterization of 1,2-diphytanoyl-sn-glycero-3-phosphocholine in model membrane systems. Biochim Biophys Acta 555:147–167. doi:10.1016/0005-2736(79)90079-8

Mäler L (2012) Solution NMR studies of peptide-lipid interactions in model membranes. Mol Membr Biol 29:155–176. doi:10.3109/09687688.2012.683456

Manzini MC, Perez KR, Riske KA, Bozelli JC Jr, Santos TL, da Silva MA, Saraiva GK, Politi MJ, Valente AP, Almeida FC, Chaimovich H, Rodrigues MA, Bemquerer MP, Schreier S, Cuccovia IM (2014) Peptide:lipid ratio and membrane surface charge determine the mechanism of action of the antimicrobial peptide BP100. Conformational and functional studies. Biochim Biophys Acta 1838:1985–1999. doi:10.1016/j.bbamem.2014.04.004

Marsh EN, Suzuki Y (2014) Using ^{19}F NMR to probe biological interactions of proteins and peptides. ACS Chem Biol 9:1242–1250. doi:10.1021/cb500111u

Matar G, Besson F (2011) Influence of the lipid composition of biomimetic monolayers on the structure and orientation of the gp41 tryptophan-rich peptide from HIV-1. Biochim Biophys Acta 1808:2534–2543. doi:10.1016/j.bbamem.2011.06.003

Mecke A, Lee DK, Ramamoorthy A, Orr BG, Banaszak Holl MM (2005) Membrane thinning due to antimicrobial peptide binding: an atomic force microscopy study of MSI-78 in lipid bilayers. Biophys J 89:4043–4050. doi:10.1529/biophysj.105.062596

Muhle-Goll C, Hoffmann S, Afonin S, Grage SL, Polyansky AA, Windisch D, Zeitler M, Bürck J, Ulrich AS (2012) Hydrophobic matching controls the tilt and stability of the dimeric platelet-derived growth factor receptor (PDGFR) β transmembrane segment. J Biol Chem 287:26178–26186. doi:10.1074/jbc.M111.325555

Naito A (2009) Structure elucidation of membrane-associated peptides and proteins in oriented bilayers by solid-state NMR spectroscopy. Solid State Nucl Magn Reson 36:67–76. doi:10.1016/j.ssnmr.2009.06.008

Neale C, Hsu JC, Yip CM, Pomès R (2014) Indolicidin binding induces thinning of a lipid bilayer. Biophys J 106:L29–L31. doi:10.1016/j.bpj.2014.02.031

Ouellet M, Doucet JD, Voyer N, Auger M (2007) Membrane topology of a 14-mer model amphipathic peptide: a solid-state NMR spectroscopy study. Biochemistry 46:6597–6606. doi:10.1021/bi0620151

Perrin BS Jr, Sodt AJ, Cotten ML, Pastor RW (2014) The curvature induction of surface-bound antimicrobial peptides piscidin 1 and piscidin 3 varies with lipid chain length. J Membr Biol. doi:10.1007/s00232-014-9733-1

Petrache HI, Dodd SW, Brown MF (2000) Area per lipid and acyl length distributions in fluid phosphatidylcholines determined by ^{2}H NMR spectroscopy. Biophys J 79:3172–3192. doi:10.1016/S0006-3495(00)76551-9

Schrank E, Wagner GE, Zangger K (2013) Solution NMR studies on the orientation of membrane-bound peptides and proteins by paramagnetic probes. Molecules 18:7407–7435. doi:10.3390/molecules18077407

Shai Y (1999) Mechanism of the binding, insertion and destabilization of phospholipid bilayer membranes by alpha-helical antimicrobial and cell non-selective membrane-lytic peptides. Biochim Biophys Acta 1462:55–70. doi:10.1016/S0005-2736(99)00200-X

Strandberg E, Tiltak D, Ehni S, Wadhwani P, Ulrich AS (2012) Lipid shape is a key factor for membrane interactions of amphipathic helical peptides. Biochim Biophys Acta 1818:1764–1776. doi:10.1016/j.bbamem.2012.02.027

Strandberg E, Zerweck J, Wadhwani P, Ulrich AS (2013) Synergistic insertion of antimicrobial magainin-family peptides in membranes depends on the lipid spontaneous curvature. Biophys J 104:L9–L11. doi:10.1016/j.bpj.2013.01.047

Su Y, Li S, Hong M (2013) Cationic membrane peptides: atomic-level insight of structure–activity relationships from solid-state NMR. Amino Acids 44:821–833. doi:10.1007/s00726-012-1421-9

Tremouilhac P, Strandberg E, Wadhwani P, Ulrich AS (2006) Conditions affecting the re-alignment of the antimicrobial peptide PGLa in membranes as monitored by solid state ^{2}H-NMR. Biochim Biophys Acta 1758:1330–1342. doi:10.1016/j.bbamem.2006.02.029

Ulrich AS (2005) Solid state ^{19}F-NMR methods for studying biomembranes. Prog NMR Spectr 46:1–21. doi:10.1016/j.pnmrs.2004.11.001

Wadhwani P, Strandberg E, Heidenreich N, Bürck J, Fanghänel S, Ulrich AS (2012a) Self-assembly of flexible β-strands into immobile amyloid-like β-sheets in membranes as revealed by solid-state ^{19}F NMR. J Am Chem Soc 134:6512–6515. doi:10.1021/ja301328f

Wadhwani P, Epand RF, Heidenreich N, Bürck J, Ulrich AS (2012b) Membrane-active peptides and the clustering of anionic lipids. Biophys J 103:265–274. doi:10.1016/j.bpj.2012.06.004

Wadhwani P, Reichert J, Strandberg E, Bürck J, Misiewicz J, Afonin S, Heidenreich N, Fanghänel S, Mykhailiuk PK, Komarov IV, Ulrich AS (2013) Stereochemical effects on the aggregation and biological properties of the fibril-forming peptide $[KIGAKI]_3$ in membranes. Phys Chem Chem Phys 15:8962–8971. doi:10.1039/c3cp50896j

Wadhwani P, Strandberg E, van den Berg J, Mink C, Bürck J, Ciriello RAM, Ulrich AS (2014) Dynamical structure of the short multifunctional peptide BP100 in membranes. Biochim Biophys Acta 1838:940–949. doi:10.1016/j.bbamem.2013.11.001

Wadhwani P, Strandberg E, Mink C, Bürck J, van den Berg J, Ciriello RAM, Reichert J, Wacker-Schröder I, Bardají E, Castanho MARB, Ulmschneider JP, Ulrich AS (2015) Multifunctionality of the short membrane-active peptide BP100, and comparison with the Magainin- and TAT families (in preparation)

Wang Y, Zhao T, Wei D, Ulrich AS, Strandberg E, Ulmschneider JP (2014) How reliable are molecular dynamics simulations of membrane active antimicrobial peptides? Biochim Biophys Acta 1838:2280–2288. doi:10.1016/j.bbamem.2014.04.009

Yang P, Wu FG, Chen Z (2013) Lipid fluid-gel phase transition induced alamethicin orientational change probed by sum frequency generation vibrational spectroscopy. J Phys Chem C Nanomater Interfaces 117:17039–17049. doi:10.1021/jp4047215

Yi HY, Chowdhury M, Huang YD, Yu XQ (2014) Insect antimicrobial peptides and their applications. Appl Microbiol Biotechnol 98:5807–5822. doi:10.1007/s00253-014-5792-6

Zairi A, Tangy F, Bouassida K, Hani K (2009) Dermaseptins and magainins: antimicrobial peptides from frogs' skin-new sources for a promising spermicides microbicides-a mini review. J Biomed Biotechnol 2009:452567. doi:10.1155/2009/452567

Zhang S, Wu XL, Mehring M (1990) Elimination of ringing effects in multiple-pulse sequences. Chem Phys Lett 173:481–484. doi:10.1016/0009-2614(90)87239-N

Zhou HX, Cross TA (2013) Influences of membrane mimetic environments on membrane protein structures. Annu Rev Biophys 42:361–392. doi:10.1146/annurev-biophys-083012-130326